

Multimode vibrational effects in single molecule conductance: A nonequilibrium Green's function approach

R. Härtle, C. Benesch, and M. Thoss

*Department of Chemistry, Technical University of Munich,
Lichtenbergstr. 4, D-85747 Garching, Germany*

(Dated: February 9, 2022)

Abstract

The role of multimode vibrational dynamics in electron transport through single molecule junctions is investigated. The study is based on a generic model, which describes charge transport through a single molecule that is attached to metal leads. To address vibrationally-coupled electron transport, we employ a nonequilibrium Green's function approach that extends a method recently proposed by Galperin et al. [Phys. Rev. B **73**, 045314 (2006)] to multiple vibrational modes. The methodology is applied to two systems: a generic model with two vibrational degrees of freedom and benzenedibutanethiolate covalently bound to gold electrodes. The results show that the coupling to multiple vibrational modes can have a significant effect on the conductance of a molecular junction. In particular, we demonstrate the effect of electronically induced coupling between different vibrational modes and study nonequilibrium vibrational effects by calculating the current-induced excitation of vibrational modes.

PACS numbers: 85.65.+h, 71.38.-k, 73.23.-b

I. INTRODUCTION

Experimental studies of single molecule conductance^{1,2,3,4} have revealed a wealth of interesting transport phenomena and have stimulated great interest in the basic mechanisms that determine electron transport on the molecular scale.^{5,6,7} Thereby, effects due to coupling between electronic and nuclear degrees of freedom have been of particular interest.⁸ The small size and the low mass of molecules may result in strong coupling between electronic and nuclear degrees of freedom.^{9,10} Vibrational structures in molecular conductance have been observed for a variety of different systems.^{9,11,12,13,14,15,16,17,18,19} Electronic-vibrational coupling can result in excitation of the vibrational modes of the molecular bridge as well as local heating.¹⁵ Conformational changes of the geometry of the conducting molecule are possible mechanisms for switching behavior and negative differential resistance²⁰. Furthermore, the observation of vibrational structures in conductance measurements allows the unambiguous identification of the molecule in the junction.

These experimental findings have inspired great interest in the theoretical modeling and simulation of vibrationally-coupled charge transport in molecular junctions.^{8,21,22,23,24,25,26,27,28,29,30,31,32,33,34,35,36,37} A variety of different approaches have been used to study the influence of the vibrational degrees of freedom on single molecule conductance, including inelastic scattering theory, density matrix approaches and nonequilibrium Green's function methods. Green's functions are particularly well-suited to study many-body and vibrational nonequilibrium effects. Employing perturbation theory, nonequilibrium Green's function methods have been applied in the off-resonant tunneling regime to study, e.g., inelastic tunneling spectra.^{25,26,36} In this regime, the effective electronic-vibrational coupling is typically small and perturbation theory valid. Galperin et al. have recently proposed a method that allows the study of vibrational effects in the resonant transport regime.³³ This method is based on a polaron transformation of the Hamiltonian and employs perturbation theory within a self-consistent scheme to solve the equations of motion for the nonequilibrium Green's function.

In the original formulation,³³ the method of Galperin et al. is limited to the treatment of a single vibrational mode that is coupled to a thermal bath. In this paper, we extend this Green's function method to allow the treatment of several vibrational degrees of freedom. Moreover, we outline a scheme that allows the calculation of current-induced vibrational

excitation and thus to study vibrational nonequilibrium effects. The methodology is applied to two different systems: a generic model of a molecular junction with two active vibrational modes as well as charge transport through benzenedibutanethiolate covalently bound to gold electrodes based on a recently developed³⁸ first-principles model.

II. THEORY

A. Model

To study vibrationally-coupled electron transport through a molecular junction, we consider a generic tight-binding model,^{33,39} where a single electronic state localized on the molecule is coupled to respective states in the left (L) and right (R) leads by tunneling matrix elements V_k ,

$$\begin{aligned}
H = & \epsilon_0 c^\dagger c + \sum_{k \in \text{L,R}} \epsilon_k c_k^\dagger c_k + \sum_{k \in \text{L,R}} (V_k c_k^\dagger c + V_k^* c^\dagger c_k) \\
& + \sum_{\alpha} \Omega_{\alpha} a_{\alpha}^{\dagger} a_{\alpha} + \sum_{\alpha} \lambda_{\alpha} Q_{\alpha} (c^{\dagger} c - \delta) + \sum_{\beta} \omega_{\beta} b_{\beta}^{\dagger} b_{\beta} + \sum_{\alpha\beta} Q_{\alpha} U_{\alpha\beta} Q_{\beta}.
\end{aligned} \tag{2.1}$$

Here, c_k^{\dagger} and c^{\dagger} are operators that create an electron in the leads and on the molecular bridge, respectively, and ϵ_k , ϵ_0 denote the energies of the corresponding electronic states. The nuclear degrees of freedom of the molecule are described in Eq. (2.1) within the harmonic approximation employing the normal modes of the neutral junction in equilibrium at zero bias. Thereby, a_{α}^{\dagger} denotes the creation operator for a normal mode of the neutral molecule with frequency Ω_{α} and $Q_{\alpha} = (a_{\alpha} + a_{\alpha}^{\dagger})$ is the corresponding displacement operator.

If an external bias is applied to the junction, electrons will be transferred from the leads to the junction and vice versa. Accordingly, the potential energy for the nuclei will be distorted. The corresponding interaction potential is approximated employing a linear expansion in the displacement operator Q_{α} around the equilibrium geometry of the neutral junction, resulting in the electronic-vibrational interaction term $\sum_{\alpha} \lambda_{\alpha} Q_{\alpha} (c^{\dagger} c - \delta)$ in Eq. (2.1). The charge density, to which this interaction potential is linked, depends on whether the molecular state through which the transport takes place is unoccupied in equilibrium ($\delta = 0$, corresponding, e.g., to charge transport through the LUMO) or occupied ($\delta = 1$, corresponding, e.g., to the HOMO).⁴⁰ The corresponding shift in the equilibrium geometry of mode α is given by $\Delta Q_{\alpha} = 2\lambda_{\alpha}/\Omega_{\alpha}$.

To account for the effect of relaxation of the vibrational modes, induced by anharmonic interactions and coupling to phonons in the electrodes, we adopt a linear response model for vibrational relaxation.^{33,39} Within this model, the normal modes of the molecule are coupled linearly in Eq. (2.1) to a thermal bath of secondary modes. Thereby, b_β^\dagger denotes the creation operator for a bath mode with frequency ω_β and $U_{\alpha\beta}$ determines the system-bath coupling strength. All properties of the bath, which influence the dynamics of the system are characterized by the spectral density⁴¹

$$J_\alpha(\omega) = \sum_{\beta} |U_{\alpha\beta}|^2 \delta(\omega - \omega_\beta). \quad (2.2)$$

In the applications considered below, we have used an Ohmic spectral density

$$J_\alpha(\omega) = \eta_\alpha \omega e^{-\omega/\omega_{c\alpha}}. \quad (2.3)$$

Here, the characteristic frequency $\omega_{c\alpha}$ defines the maximum of the spectral density and the overall coupling strength is determined by η_α . Both values may depend on the specific system mode α .

To apply (self-consistent) perturbation theory within the nonequilibrium Green's functions approach considered below, it is expedient to remove the direct coupling terms between electrons and vibrations in the Hamiltonian, $\lambda_\alpha Q_\alpha (c^\dagger c - \delta)$. To this end, we apply a standard canonical transformation, also referred to as Lang-Firsov (or small polaron) transformation^{42,43}

$$\begin{aligned} \overline{H} &\equiv e^S H e^{-S}, \\ &= \bar{\epsilon}_0 c^\dagger c + \sum_{k \in \text{L,R}} \epsilon_k c_k^\dagger c_k + \sum_{k \in \text{L,R}} (V_k X c_k^\dagger c + V_k^* X^\dagger c^\dagger c_k) \\ &\quad + \mathbf{A}^\dagger \mathbf{W}_a \mathbf{A} + \mathbf{B}^\dagger \mathbf{W}_b \mathbf{B} + \mathbf{Q}_a^\dagger \mathbf{U} \mathbf{Q}_b, \end{aligned} \quad (2.4)$$

with $X = \exp(i\mathbf{P}_a^\dagger \mathbf{W}_a^{-1} \mathbf{\Lambda})$ and $S = -i\mathbf{P}_a^\dagger \mathbf{W}_a^{-1} \mathbf{\Lambda} (c^\dagger c - \delta)$. For notational convenience we introduce the vectors $(\mathbf{Q}_a)_\alpha = Q_\alpha$, $(\mathbf{P}_a)_\alpha = -i(a_\alpha - a_\alpha^\dagger)$, $(\mathbf{A})_\alpha = a_\alpha$, $(\mathbf{\Lambda})_\alpha = \lambda_\alpha$, the matrices $(\mathbf{W}_a)_{\alpha\alpha'} = \delta_{\alpha\alpha'} \Omega_\alpha$, $(\mathbf{U})_{\alpha\beta} = U_{\alpha\beta}$, as well as respective quantities for the bath modes. It is noted that, in the presence of a bath, the decoupling requires that the eigenvalues of the matrix $(4\mathbf{U}\mathbf{W}_b^{-1}\mathbf{U}^\dagger\mathbf{W}_a^{-1})$ are smaller than unity,³³ corresponding to weak system-bath coupling.

The electronic-vibrational coupling manifests itself in the transformed Hamiltonian (2.4) in a polaron shift of the electronic energy

$$\epsilon_0 \rightarrow \bar{\epsilon}_0 = \begin{cases} \epsilon_0 - \mathbf{\Lambda}^\dagger \mathbf{W}_a^{-1} \mathbf{\Lambda}, & \delta = 0, \\ \epsilon_0 + \mathbf{\Lambda}^\dagger \mathbf{W}_a^{-1} \mathbf{\Lambda}, & \delta = 1, \end{cases} \quad (2.5)$$

and in the shift generator X that dresses the molecule-lead couplings V_k .

B. Nonequilibrium Green's function approach

To describe transport properties for the model introduced above, we employ a nonequilibrium Green's function method, which was proposed by Galperin et al.³³ Here, we generalize this method for applications to multiple vibrational system modes and outline how this method can be used to calculate vibrational properties.

The central quantity in nonequilibrium Green's function theory is the electronic Green's function on the molecular bridge

$$\begin{aligned} G(\tau, \tau') &= -i \langle T_c c(\tau) c^\dagger(\tau') \rangle_H, \\ &= -i \langle T_c c(\tau) c^\dagger(\tau') X(\tau) X^\dagger(\tau') \rangle_{\bar{H}}, \end{aligned} \quad (2.6)$$

where T_c denotes the time-ordering operator along the Keldysh contour⁴⁴ and the subscripts H/\bar{H} indicate the Hamiltonian that is used in the calculation of the respective expectation value. Most expectation values considered below refer to \bar{H} , for which the corresponding subscript is omitted in the following.

Following Galperin et al.,³³ the electronic Green's function $G(\tau, \tau')$ is factorized,

$$G(\tau, \tau') \approx G_c(\tau, \tau') \langle T_c X(\tau) X^\dagger(\tau') \rangle, \quad (2.7)$$

into a correlation function of the shift generator, $\langle T_c X(\tau) X^\dagger(\tau') \rangle$, and an electronic Green's function, $G_c(\tau, \tau')$, with

$$G_c(\tau, \tau') = -i \langle T_c c(\tau) c^\dagger(\tau') \rangle_{\bar{H}}. \quad (2.8)$$

This factorization is valid in the limit of weak molecule-lead coupling corresponding to a relatively long residence time of the electron on the molecular bridge. This is the regime, where vibrational effects are expected to be particularly pronounced.³⁸

Based on the Hamiltonian \overline{H} and employing the equation of motion for the electronic Green's function, the following equation for $G_c(\tau, \tau')$ is obtained^{33,45}

$$G_c(\tau, \tau') = G_c^0(\tau, \tau') + \int d\tau_1 d\tau_2 G_c^0(\tau, \tau_1) \Sigma_c(\tau_1, \tau_2) G_c^0(\tau_2, \tau'), \quad (2.9)$$

where G_c^0 denotes the electronic Green's function for vanishing electronic coupling (i.e. $V_k = 0$). The self energy $\Sigma_c(\tau, \tau')$, introduced in Eq. (2.9), comprises all interactions of the electronic degrees of freedom on the molecule with those in the leads and the vibrational modes and is given by

$$\begin{aligned} \Sigma_c(\tau, \tau') &= \sum_{k \in \text{L,R}} |V_k|^2 g_k(\tau, \tau') \langle T_c X(\tau') X^\dagger(\tau) \rangle, \\ &\equiv \Sigma_c^0(\tau, \tau') \langle T_c X(\tau') X^\dagger(\tau) \rangle, \end{aligned} \quad (2.10)$$

with $g_k = -i \langle T_c c_k(\tau) c_k^\dagger(\tau') \rangle$. The above expression holds to second order in V_k , i.e. for weak molecule-lead coupling.

To extend the validity to moderate coupling, which is particularly important to describe vibrational effects in resonant electron transport, higher order terms are taken into account. To this end, a self-consistent scheme is introduced by replacing the last G_c^0 in the integral kernel of Eq. (2.9) by G_c ,^{33,45}

$$G_c(\tau, \tau') = G_c^0(\tau, \tau') + \int d\tau_1 d\tau_2 G_c^0(\tau, \tau_1) \Sigma_c(\tau_1, \tau_2) G_c(\tau_2, \tau'). \quad (2.11)$$

It is noted that Eq. (2.11) gives the exact electronic Green's function for vanishing electronic-vibrational coupling (i.e. $\lambda_\alpha = 0$).

Projection of Eq. (2.11) onto the real time axis, according to analytic continuation rules,⁴⁶ and Fourier transformation of the resulting equations gives a Dyson equation

$$G_c^r(E) = G_c^{0,r} + G_c^{0,r}(E) \Sigma_c^r(E) G_c^r(E), \quad (2.12a)$$

and a Keldysh equation

$$G_c^<(E) = G_c^r(E) \Sigma_c^<(E) G_c^a(E), \quad (2.12b)$$

where we have introduced the retarded (G_c^r), advanced (G_c^a), and lesser ($G_c^<$) Green's functions and the corresponding self energies. It should be emphasized that the derivation of the compact form of these equations requires time-translational invariance and the existence of a steady-state transport regime.

So far, we have only considered the electronic part of the Green's function $G(\tau, \tau')$. The solution of the equations requires also the calculation of the shift generator correlation function $\langle T_c X(\tau) X^\dagger(\tau') \rangle$. Using a cumulant expansion up to second order in the vibronic coupling parameters $\lambda_\alpha/\Omega_\alpha$ yields^{33,42}

$$\langle T_c X(\tau) X^\dagger(\tau') \rangle = \exp \left[i \mathbf{\Lambda}^\dagger \mathbf{W}_a^{-1} (\mathbf{D}(\tau, \tau') - \mathbf{D}(\tau, \tau)) \mathbf{W}_a^{-1} \mathbf{\Lambda} \right], \quad (2.13)$$

where $\mathbf{D}(\tau, \tau') = -i \langle T_c \mathbf{P}_a(\tau) \mathbf{P}_a^\dagger(\tau') \rangle$ denotes the correlation matrix of the momentum vector \mathbf{P}_a , in the following referred to as the vibrational Green's function. In the limit $V_k \rightarrow 0$, Eq. (2.13) constitutes an analytically exact expression. Employing again an equation of motion approach, one can derive Dyson/Keldysh equations for the vibrational Green's function $\mathbf{D}(\tau, \tau')$. The resulting self energy term $\mathbf{\Pi}_{\text{el}}(\tau, \tau')$ describes interactions between electrons and vibrations. This self energy was obtained by Galperin et al. for a single vibrational mode.³³ Employing the same level of approximations, we obtain for multiple vibrational modes

$$\mathbf{\Pi}_{\text{el}}(\tau, \tau') = -i \mathbf{W}_a^{-1} \mathbf{\Lambda} \mathbf{\Lambda}^\dagger \mathbf{W}_a^{-1} (\Sigma_c(\tau, \tau') G_c(\tau', \tau) + \Sigma_c(\tau', \tau) G_c(\tau, \tau')), \quad (2.14)$$

and

$$\mathbf{D}^r(E) = \mathbf{D}^{0,r} + \mathbf{D}^{0,r}(E) \mathbf{\Pi}_{\text{el}}^r(E) \mathbf{D}^r(E), \quad (2.15a)$$

$$\mathbf{D}^<(E) = \mathbf{D}^r(E) \mathbf{\Pi}_{\text{el}}^<(E) \mathbf{D}^a(E). \quad (2.15b)$$

The off-diagonal elements of the self energy matrix $\mathbf{\Pi}_{\text{el}}$ describe interactions between different vibrational modes mediated by the electronic degrees of freedom. The matrix \mathbf{D}^0 describes momentum correlations of the vibrations in thermal equilibrium and plays the same role for the vibrational Green's function \mathbf{D} as G_c^0 for the electronic Green's function G_c . In the presence of a thermal bath, the matrix \mathbf{D}^0 need not to be of diagonal form, especially if the bath degrees of freedom couple the various vibrational modes with each other.

The equations for the electronic and vibrational Green's functions outlined above have to be solved self-consistently. We employ the following self-consistent scheme:³³ As a starting point we use the free electronic and vibrational Green's functions. The free vibrational Green's function \mathbf{D}^0 enters the shift generator correlation function according to Eq. (2.13). Next, the shift generator correlation function is convoluted with the bare self energy Σ_c^0 ,

which gives the dressed self energy Σ_c according to Eq. (2.10). The dressed self energy Σ_c , which now contains interactions of the electronic degrees of freedom on the molecule with both the leads and the vibrations, is inserted into the electronic Green's function G_c , Eqs. (2.12), and into the self energy term $\mathbf{\Pi}_{\text{el}}$ of the vibrational Green's function, Eq. (2.14). The new Green's function \mathbf{D} is obtained from the Dyson/Keldysh equations (2.15), and enters the shift generator correlation function. Thus, the self-consistent cycle closes, and all steps can be repeated with the updated shift generator correlation function. Convergence is reached as soon as the variation of the electronic occupation number, $n_c = \text{Im}[G_c^<(t=0)]$, between subsequent iteration steps falls below a threshold of 10^{-7} . This way, we obtain self-consistent solutions of Eqs. (2.12) and (2.15).

C. Observables of interest

Several observables can be considered to study the effects of vibrational motion on charge transport through single molecule junctions. Here, we will focus on the current-voltage characteristic, the differential conductance and the vibrational nonequilibrium distribution.

Based on the self-consistent result for the Green's function, the current through lead K ($K \in \{\text{L}, \text{R}\}$) induced by an external dc-bias Φ is obtained employing the formula of Meir, Wingreen and Jauho^{45,47,48}

$$I_K = \frac{2e}{\hbar} \int \frac{dE}{2\pi} [\Sigma_{c,K}^<(E)G_c^>(E) - \Sigma_{c,K}^>(E)G_c^<(E)], \quad (2.16)$$

with

$$\begin{aligned} \Sigma_{c,K}(\tau, \tau') &= \sum_{k \in K} |V_k|^2 g_k(\tau, \tau') \langle T_c X(\tau') X^\dagger(\tau) \rangle, \\ &\equiv \Sigma_{c,K}^0(\tau, \tau') \langle T_c X(\tau') X^\dagger(\tau) \rangle. \end{aligned} \quad (2.17)$$

Thereby, the factor two accounts for spin degeneracy. The differential conductance is given by $g = dI/d\Phi$.

It is noted that the scheme outlined above conserves the number of electrons and thus obeys Kirchhoff's law, $I_L = -I_R$. Furthermore, as there is no direct electron-vibrational coupling term in the Hamiltonian \overline{H} , the symmetrized current $I = 1/2(I_L - I_R)$ can be expressed in terms of a transmission function $\mathcal{T}(E)$

$$I = \frac{2e}{\hbar} \int \frac{dE}{2\pi} (f_L(E) - f_R(E)) \mathcal{T}(E), \quad (2.18)$$

with

$$\mathcal{T}(E) = \frac{\Gamma_L(E)\Gamma_R(E)}{\Gamma_L(E) + \Gamma_R(E)} i (G_c^r(E) - G_c^a(E)). \quad (2.19)$$

Here, we have introduced the nonequilibrium distribution function

$$f_K(E) = \frac{\text{Im}[\Sigma_{c,K}^<(E)]}{\Gamma_K(E)}, \quad (2.20)$$

and the width function

$$\Gamma_K(E) = -2\text{Im}[\Sigma_{c,K}^r(E)]. \quad (2.21)$$

Another interesting observable to investigate vibrationally-coupled electron transport in molecular junctions is the nonequilibrium vibrational distribution. Due to current-induced excitation and deexcitation of the vibrational modes, the vibrational distribution in the stationary state may differ significantly from its equilibrium distribution. To study such vibrational nonequilibrium effects, we consider in this work the average occupation number of different vibrational modes

$$n_\alpha = \langle a_\alpha^\dagger a_\alpha \rangle_H. \quad (2.22)$$

Within the self-consistent Green's function approach employed here, n_α is given (up to second order in the system-bath interaction $U_{\alpha\beta}$) by the expression

$$n_\alpha = - \left(A_\alpha + \frac{1}{2} \right) \text{Im}[(\mathbf{D}(t=0))_{\alpha\alpha}] - \left(B_\alpha + \frac{1}{2} \right) + \frac{\lambda_\alpha^2}{\Omega_\alpha^2} \begin{cases} n_c, & \delta = 0, \\ 1 - n_c, & \delta = 1, \end{cases} \quad (2.23)$$

with

$$A_\alpha = \sum_\beta \frac{U_{\alpha\beta}^2 \omega_\beta}{\Omega_\alpha(\omega_\beta^2 - \Omega_\alpha^2)}, \quad (2.24a)$$

$$B_\alpha = \sum_\beta \frac{U_{\alpha\beta}^2}{(\omega_\beta^2 - \Omega_\alpha^2)} (1 + 2N_B(\omega_\beta)). \quad (2.24b)$$

Thereby, $n_c = \langle c^\dagger c \rangle_H$ denotes the stationary population of the molecular electronic state. The derivation of Eq. (2.23) is outlined in the Appendix.

III. RESULTS AND DISCUSSION

The methodology outlined above has been applied to two different systems: A generic model for a molecular junction including two vibrational modes and charge transport through benzenedibutanethiolate coupled to gold electrodes. In the latter system the four most strongly coupled vibrational modes have been taken into account.

A. Generic model system with two vibrational degrees of freedom

First, we consider a generic model system with a single molecular orbital coupled to two vibrational degrees of freedom. The energy of the molecular state is chosen as $\epsilon_0 = 1\text{ eV}$ and is located well above the Fermi energy of the leads, $\epsilon_F = 0\text{ eV}$. Thus in equilibrium, the molecular state is unoccupied (corresponding to $\delta = 0$). The leads are modelled by a one-dimensional tight-binding model with nearest-neighbor coupling constant $\beta = 2\text{ eV}$ and molecule-lead coupling strength $\nu = 0.1\text{ eV}$. This results in an unstructured semi-elliptic conduction band with self energies³⁹

$$\Sigma_{c,K}^{0,r}(E) = \Delta_K^0(E) - \frac{i}{2}\Gamma_K^0(E), \quad (3.1a)$$

$$\Sigma_{c,K}^{0,<}(E) = if_K^0(E)\Gamma_K^0(E), \quad (3.1b)$$

$$\Sigma_{c,K}^{0,>}(E) = -i(1 - f_K^0(E))\Gamma_K^0(E), \quad (3.1c)$$

where the corresponding level-width function reads

$$\Gamma_K^0(E) = \frac{\nu^2}{\beta^2} \text{Im} \left[\sqrt{(E - \mu_K)^2 - 4\beta^2} \right], \quad (3.2)$$

and Δ_K^0 is the Hilbert transform of Γ_K^0 . Furthermore, f_K^0 denotes the Fermi distribution in the leads,

$$f_K^0(E) = \frac{1}{1 + \exp\left(\frac{E - \mu_K}{k_B T}\right)}, \quad (3.3)$$

$\mu_{L(R)}$ is the chemical potential in the leads, and Φ the bias voltage. We assume the bias voltage to drop symmetrically at the right and the left contact, $\mu_{L(R)} = \epsilon_F \pm \Phi/2$. In the results presented below, we have used a temperature of $k_B T = 1\text{ meV}$. This temperature is low enough to study vibrational features undistorted by thermal fluctuations ($k_B T \ll \Omega_{1(2)}$).

The parameters of the two vibrational modes of the model are given in Tab. I. Each mode

frequency	vibronic coupling	system-bath coupling
$\Omega_1 = 0.10 \text{ eV}$	$\lambda_1 = 0.06 \text{ eV}$	$\eta_1 = 0.001$
$\Omega_2 = 0.25 \text{ eV}$	$\lambda_2 = 0.15 \text{ eV}$	$\eta_2 = 0.001$

TABLE I: Vibrational parameters of the model system with two vibrational modes.

is coupled to an Ohmic bath as described by Eqs. (2.2), (2.3). Thereby, the characteristic frequencies of the bath spectral density were chosen to coincide with the frequency of the respective system mode, i.e. $\omega_{c\alpha} = \Omega_\alpha$. A relatively weak system-bath coupling strength was used, $\eta_\alpha = 0.001$, corresponding to vibrational relaxation times of about 0.1–1 ps. In principle, the thermal bath couples the two vibrational modes with each other. This interaction is neglected in the calculation presented below. Hence, the retarded projection of the correlation matrix \mathbf{D}^0 has a diagonal form

$$\mathbf{D}_{\alpha\alpha'}^{0,r}(\omega) = \delta_{\alpha\alpha'} \frac{2\Omega_\alpha}{\omega^2 - \Omega_\alpha^2 - 2\Omega_\alpha \Pi_{\text{bath},\alpha}^r(\omega)}, \quad (3.4)$$

with

$$-2\text{Im}[\Pi_{\text{bath},\alpha}^r(\omega)] = 2\pi J_\alpha(\omega). \quad (3.5)$$

The approach presented above can be used to describe two different regimes of electron transport: inelastic electron tunneling in the off-resonant regime and inelastic resonant electron transport. Fig. 1 shows the conductance as a function of bias voltage in the inelastic electron tunneling regime, $\Phi \lesssim 1 \text{ V}$. In this off-resonant transport regime, electronic-vibrational coupling manifests itself in steps of the conductance at voltages $\Phi = \Omega_1, 2\Omega_1, \Omega_2, \dots$ that correspond to the opening of inelastic channels. These channels are related to the excitation of vibrational quanta and will be referred to as emission channels in the following. The relative step heights reflect the respective transition probabilities determined by the corresponding Franck-Condon factors. Absorptive channels, corresponding to deexcitation of vibrational quanta, play only a minor role in this regime. This is due to the low temperature and the small electric current, which is insufficient to drive the vibrational system far from equilibrium. The comparison of the results obtained with (black line) and without (gray line) vibrational self energy $\mathbf{\Pi}_{\text{el}}$ shows that in the off-resonant regime vibrational nonequilibrium effects manifest themselves in a shift of the conductance steps.

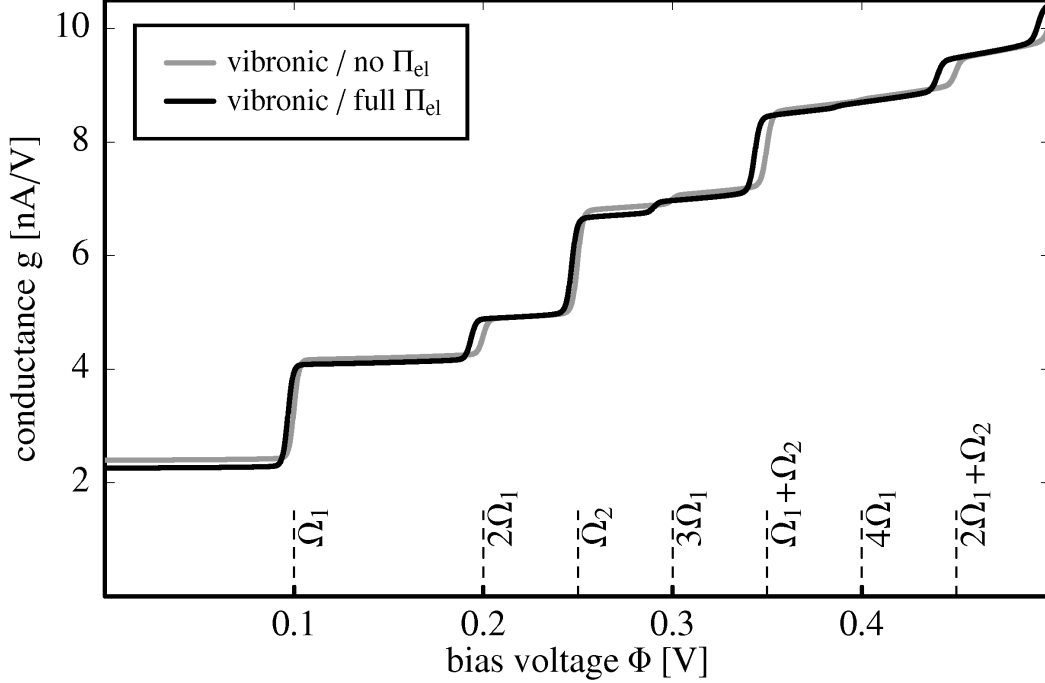


FIG. 1: Conductance g for the model with two vibrational modes in the inelastic electron tunneling regime. The solid gray line refers to a calculation with vibrations in thermal equilibrium, $\Pi_{\text{el}} = 0$, while the solid black line presents results including nonequilibrium effects, $\Pi_{\text{el}} \neq 0$. The thin dashed lines indicate the voltages corresponding to the opening of vibrationally inelastic channels.

We next consider the resonant transport regime, which is found for voltages $\Phi \gtrsim 1.5 \text{ V}$. Fig. 2 shows the current and the conductance in this regime based on three different calculations: full vibronic calculations with (solid black lines) and without (solid gray lines) vibrational nonequilibrium effects as well as results of a purely electronic calculation (i.e. $\lambda_\alpha = 0$, black dashed lines). The purely electronic calculation exhibits a single peak in the conductance at a bias voltage of $\Phi \approx 2\epsilon_0$ when the molecular level enters the conductance window between the chemical potentials of the left and the right lead ($\mu_L > \epsilon_0 > \mu_R$). The subsequent decrease of the current results from the finite width of the conduction band.³⁹

The coupling to the vibrational degrees of freedom manifests itself in steps in the current and as peaks in the conductance. For the present model ($\delta = 0$), these resonance structures can be approximately associated to transitions between the vibrational states of the neutral molecule and those of the molecular anion. Thereby, transitions from vibrational states of the neutral molecule to those of the anion dominate in the low-voltage regime, where

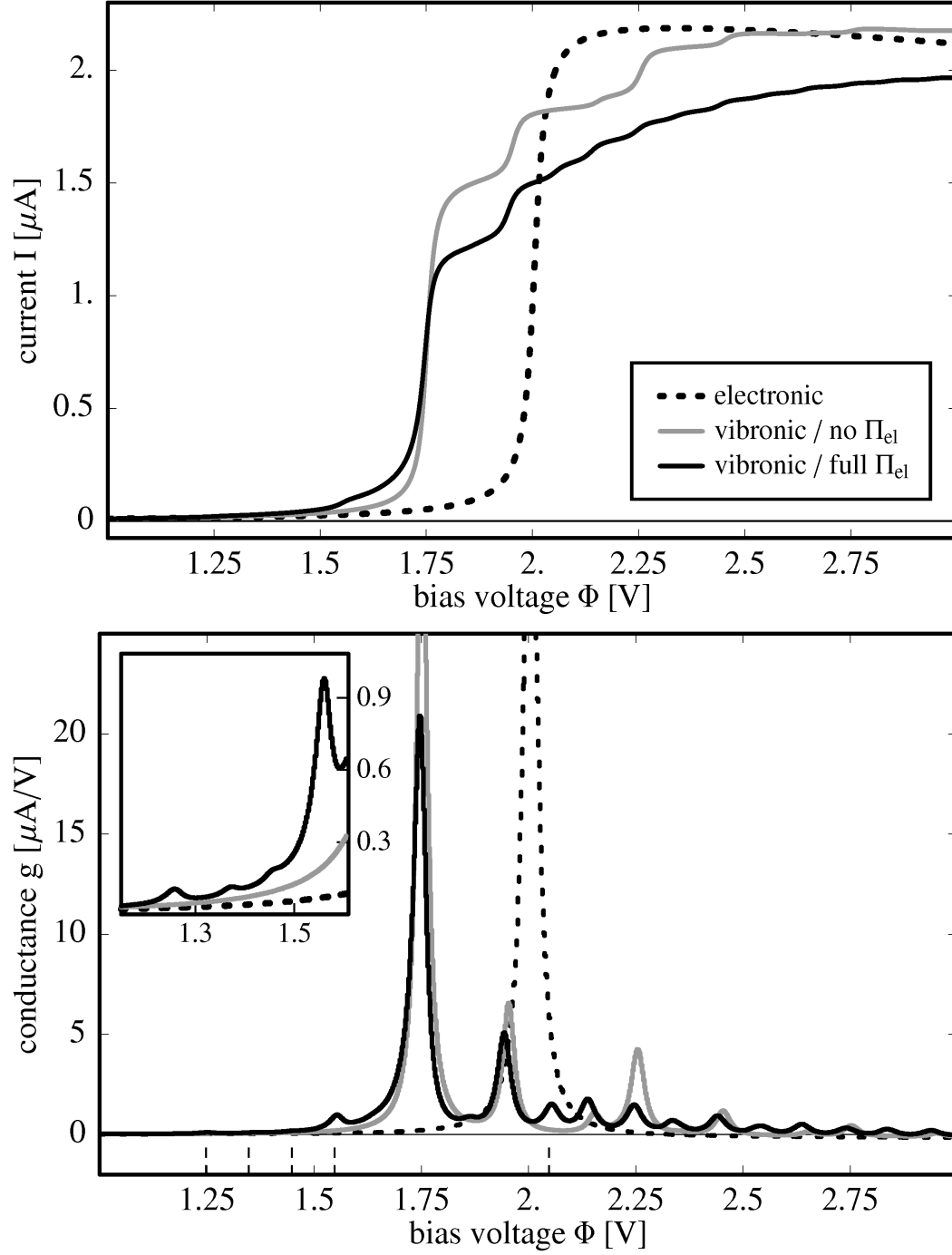


FIG. 2: Current (top) and conductance (bottom) for the model with two vibrational modes in the resonant transport regime. The dashed black line refers to a purely electronic calculation. The solid gray line depicts results with vibrations in thermal equilibrium, $\Pi_{\text{el}} = 0$, while the solid black line presents results including nonequilibrium effects, $\Pi_{\text{el}} \neq 0$.

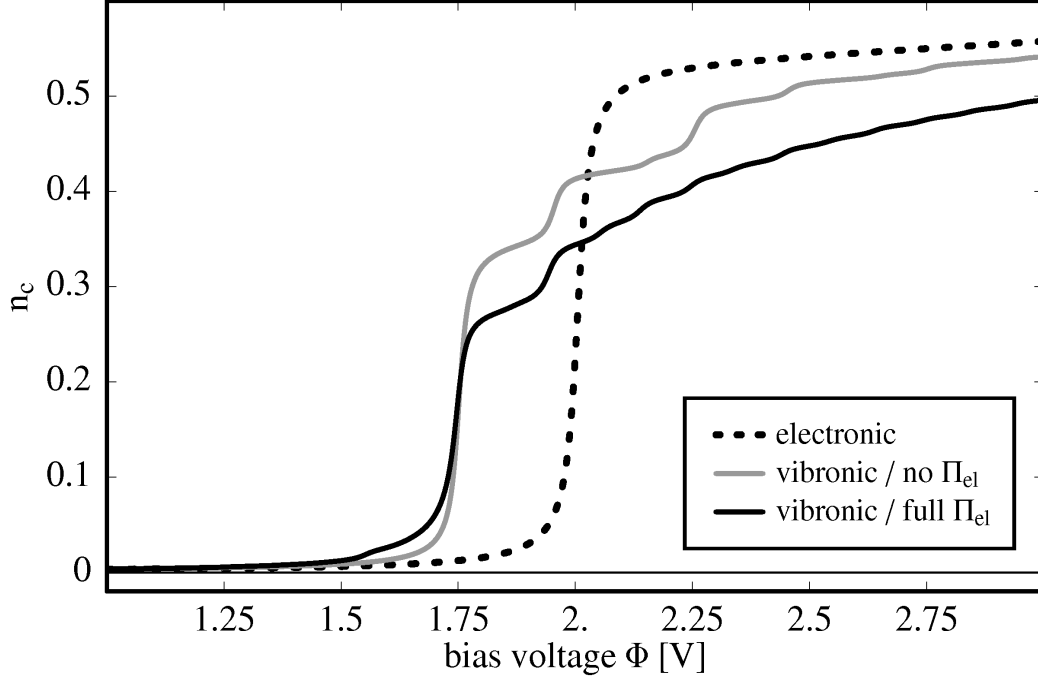


FIG. 3: Population of the electronic state, $n_c = \text{Im}[G_c^<(t=0)]$, for the model with two vibrational modes.

the electronic state on the molecular bridge is essentially unoccupied (cf. Fig. 3). For higher voltages, the electronic population on the molecular bridge is no longer negligible and, therefore, also transitions from the vibrational states in the molecular anion to those in the neutral system contribute to the current. Because, in the present model, the vibrational frequencies are the same for both electronic states, features related to these transitions appear at the same voltages and cannot straightforwardly be distinguished. The population of the electronic state is depicted in Fig. 3. The electronic population increases with bias voltage in a step-like fashion similar to the current-voltage characteristic (cf. Fig. 2(a)). In contrast to the current, which decreases for large voltages due to the finite band width, the population increases for larger voltages and exceeds the wide-band limit, which is 0.5 for a symmetric junction.

If vibrational nonequilibrium effects are neglected ($\Pi_{\text{el}} = 0$, solid gray line), the molecule is (due to the low temperature) in its vibrational ground state. Correspondingly, the transmitting electrons can only induce transitions starting from the vibrational ground state. The lowest peak in the conductance corresponds predominantly to the transition from the vibrational ground state in the neutral molecule to the vibrational ground state of the anion.

Due to the polaron shift (cf. Eq. (2.5)), which accounts for the difference between the vertical (purely electronic) and adiabatic transition energy, this peak appears at a lower bias voltage ($\Phi \approx 2\bar{\epsilon}_0$, with $\bar{\epsilon}_0 = 0.874\text{eV}$) than the peak in the purely electronic calculation. According to the moderate coupling parameters, $\lambda_{1(2)}/\Omega_{1(2)} = 0.6$, this conductance peak has the largest intensity. Several resonance structures appear at larger voltages. These structures can be approximately associated with vibrationally excited states in the molecular anion. The relative peak heights follow qualitatively the respective Franck-Condon factors. However, the intensities do not coincide with the relative Franck-Condon factors because both electron and hole transport contribute to the current.

If vibrational nonequilibrium effects are included, $\Pi_{\text{el}} \neq 0$, additional peaks appear in the conductance. These are due to the fact that the nonequilibrium stationary state of the vibrational modes is no longer the ground state but involves excited states. Thus, in addition to the transitions considered above, where the electron can only lose energy to the vibrations, the electrons may induce transitions from vibrationally higher excited states to lower vibrational states corresponding to the absorption of vibrational energy by the transmitting electrons. As a result, the current (solid black lines) increases already before the shifted electronic state enters the conductance window $[\mu_L, \mu_R]$. The four conductance peaks, which are seen in the inset of Fig. 2(b), are caused predominantly by such absorptive processes. Some of the structures involve both excitation and deexcitation of vibrational modes. For example, the peak at $\Phi \approx 1.45\text{V}$ is associated to emission of energy to mode (1) and absorption of energy from mode (2). Similar processes are found for higher voltages. The position of features that exist only due to absorptive processes is highlighted by thin dashed lines. For voltages $\Phi \gtrsim 1.75\text{V}$, the current including vibrational nonequilibrium effects is found to be smaller than the current neglecting such effects. This is in agreement with previous model studies.⁴⁹ The reduced current reflects the fact that transitions between the neutral molecule and the anion are suppressed for a vibrationally excited molecular bridge.

The findings discussed above are corroborated by Fig. 4, which shows the nonequilibrium vibrational excitation $n_{1(2)}$ in the stationary state. For voltages in the resonant regime ($\Phi > 1.5\text{V}$), the results exhibit pronounced vibrational excitation, corresponding to a significant deviation of the nonequilibrium vibrational distribution from the equilibrium distribution. Because excitation of mode (1) requires less energy than that of mode (2), and because of the equal coupling parameters $\lambda_{1(2)}/\Omega_{1(2)} = 0.6$, n_1 is systematically larger than n_2 .

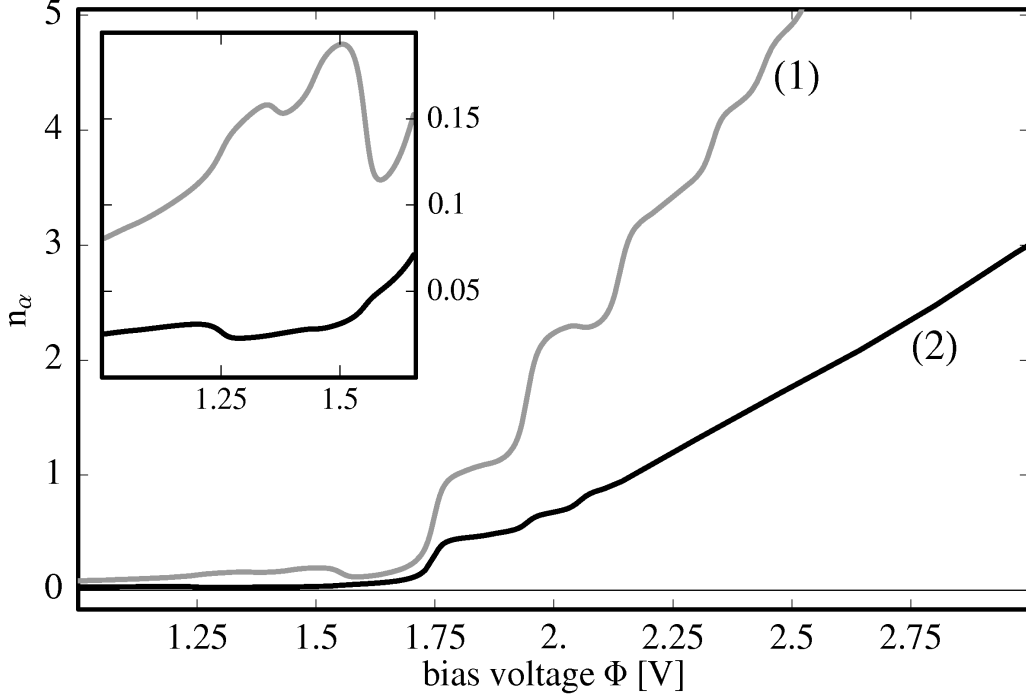


FIG. 4: Nonequilibrium vibrational excitation for the model with two vibrational modes. Solid gray lines refer to the mode with $\Omega_1 = 0.10$ eV, and the solid black lines to the one with $\Omega_2 = 0.25$ eV.

The vibrational occupation numbers exhibit steplike changes at the same bias voltages as the current.⁴⁹ In contrast to the current-voltage characteristic, however, at some steps the vibrational excitation decreases, corresponding to absorptive processes.

Finally, we discuss the coupling of the two vibrational modes mediated by the electronic degrees of freedom. Technically, this coupling is described by the off-diagonal elements of the self energy $\mathbf{\Pi}_{\text{el}}$, which depend both on the electronic molecule-lead coupling and the electronic-vibrational coupling. Because the coupling of the vibrational modes is mediated by the electronic degrees of freedom, it would enter a perturbative description only in second order. As a result, for the relatively small molecule-lead coupling considered here, large contributions are only expected for quasidegenerate vibrational modes, $\Omega_1 \approx \Omega_2$. To study this effect, Fig. 5 shows the nonequilibrium vibrational excitation of the two modes for fixed voltage ($\Phi = 3.5$ V) as a function of the frequency of mode (1). Thereby, the electronic-vibrational coupling strength λ_1 was adjusted to keep the dimensionless coupling parameter at the constant value $\lambda_1/\Omega_1 = 0.6$. All other parameters of the model remain unchanged. In addition to the results including the full self energy $\mathbf{\Pi}_{\text{el}}$ (solid lines), results neglecting the off-diagonal elements of $\mathbf{\Pi}_{\text{el}}$ are depicted (dashed lines). The results demonstrate that for

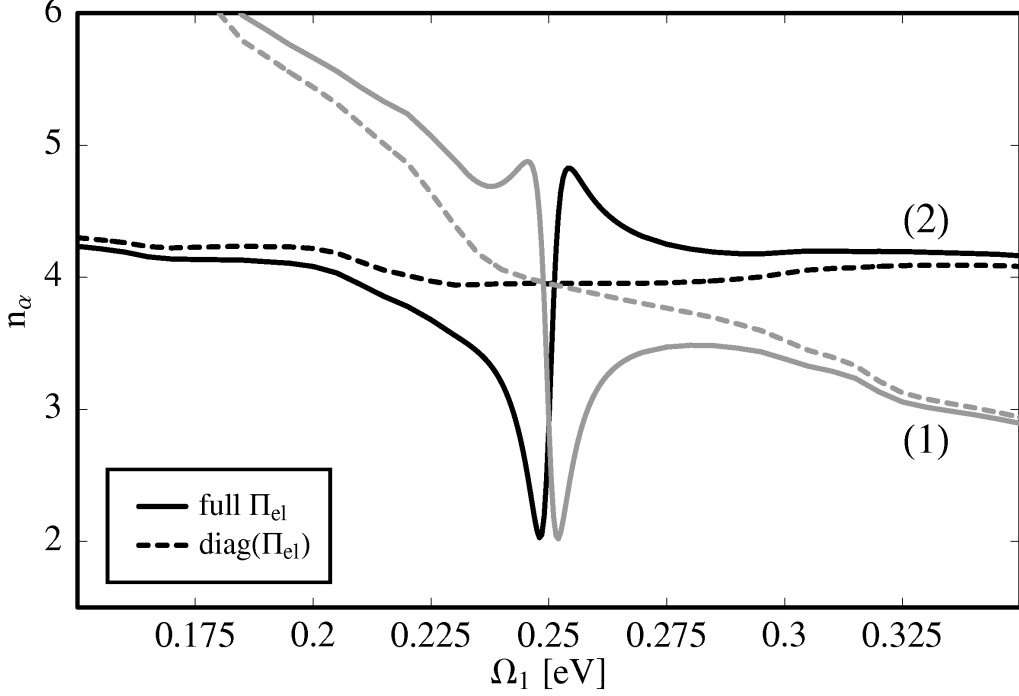


FIG. 5: Vibrational excitation numbers $n_{1(2)}$ versus the vibrational frequency Ω_1 for the model with two vibrational modes. The bias voltage is set to 3.5 V. Gray lines refer to mode (1), black lines to mode (2). Dashed lines are calculated neglecting the off-diagonal elements of $\mathbf{\Pi}_{\text{el}}$, while the solid lines are obtained using the full self energy matrix.

vibrational modes with significantly different frequencies, as considered above in Figs. 2–4, the electronically mediated mode-mode coupling has little effect and thus the off-diagonal elements of $\mathbf{\Pi}_{\text{el}}$ could be neglected. For quasidegenerate modes with similar frequencies $\Omega_1 \approx \Omega_2$, on the other hand, neglecting the off-diagonal elements of $\mathbf{\Pi}_{\text{el}}$ would result in qualitatively incorrect results. In particular, the results including the full self energy matrix predict a resonant behavior of the vibrational excitation for quasidegenerate modes, which is missed if the off-diagonal elements of the self energy $\mathbf{\Pi}_{\text{el}}$ are neglected.

It is noted, that if the modes are exactly degenerate, $\Omega_1 = \Omega_2 = \Omega$, and have the same vibronic coupling, $\lambda_1 = \lambda_2 = \lambda$, the system can be equivalently represented by a single vibrational mode with energy Ω and coupling parameter $\sqrt{2}\lambda$ (or $\sqrt{N}\lambda$ for N degenerate modes). Calculating the excitation number n_{single} for this single mode system, we obtain $n_{\text{single}} \approx n_1 + n_2 = 2n_{1(2)}$. The agreement of n_{single} with $2n_{1(2)}$ corroborates the approximations employed in the derivation of Eq. (2.23).

frequency	vibronic coupling in state A	vibronic coupling in state B	system-bath coupling
$\Omega_a = 0.070 \text{ eV}$	$\lambda_a^{(A)} = 0.021 \text{ eV}$	$\lambda_a^{(B)} = 0.049 \text{ eV}$	$\eta_a = 0.001$
$\Omega_b = 0.149 \text{ eV}$	$\lambda_b^{(A)} = 0.052 \text{ eV}$	$\lambda_b^{(B)} = 0.037 \text{ eV}$	$\eta_b = 0.001$
$\Omega_c = 0.153 \text{ eV}$	$\lambda_c^{(A)} = 0.039 \text{ eV}$	$\lambda_c^{(B)} = 0.080 \text{ eV}$	$\eta_c = 0.001$
$\Omega_d = 0.208 \text{ eV}$	$\lambda_d^{(A)} = 0.120 \text{ eV}$	$\lambda_d^{(B)} = 0.093 \text{ eV}$	$\eta_d = 0.001$

TABLE II: Vibrational parameters for the benzenedibutanethiolate molecular junction.

B. Benzenedibutanethiolate

As a second application, we consider electron transport through *p*-benzene-di(butanethiolate) (BDBT) bound to gold electrodes. This system was chosen because the butyl spacer group acts as an insulator between the electronic π -system of benzene and the gold electrodes. Compared to benzenedithiolate,⁵⁰ the residence time of the electron on the molecular bridge is thus significantly longer, which results in pronounced vibrational effects. In recent work, we have developed a first-principles model to describe vibrationally-coupled electron transport through BDBT and studied conductance properties employing inelastic scattering theory.³⁸ Here, we apply the nonequilibrium Green's function approach outlined above to investigate charge transport through BDBT.

The details of the model are described in Ref. 38. Briefly, electron transport through BDBT is dominated by two electronic states localized at the molecular bridge (denoted A and B in the following). The energies of these two states are located at $\epsilon_A = -1.38 \text{ eV}$, $\epsilon_B = -1.77 \text{ eV}$ with respect to the Fermi energy of the junction. As a result, the states are occupied in equilibrium, corresponding to $\delta = 1$. The model includes the four most strongly coupled vibrational modes. The parameters of these modes are given in Tab. II. Vibrational relaxation is described in the same manner as for the model system considered above.

Strictly speaking, the nonequilibrium approach outlined above can only be applied to a single electronic state on the molecular bridge. The extension of the approach to allow the description of multiple electronic states will be the subject of future work. In the system considered here, the electronic states are well separated from each other (with respect to the corresponding level broadening, Γ_K), and, furthermore, at least three vibrational quanta are required to bridge the electronic energy gap, $\bar{\epsilon}_A - \bar{\epsilon}_B \approx 0.37 \text{ eV}$. Therefore, we neglect coherences between the two electronic states and calculate the overall current as the sum of

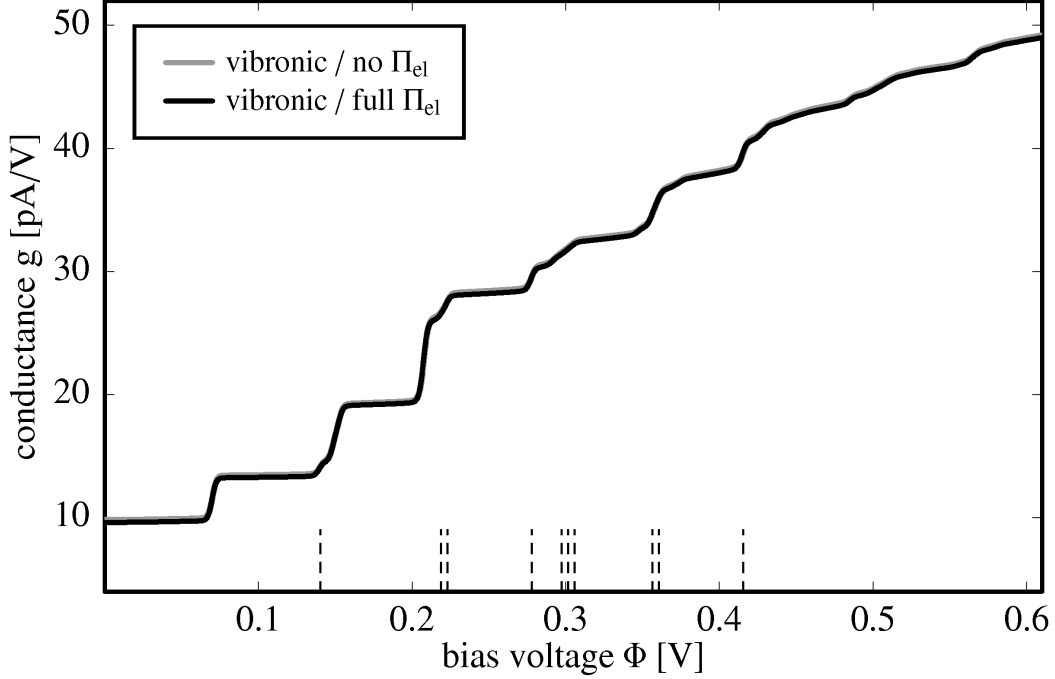


FIG. 6: Conductance of a benzenedibutanethiolate molecular junction in the inelastic tunneling regime. The solid gray line refers to a calculation with vibrations in thermal equilibrium, $\Pi_{\text{el}} = 0$, while the solid black line presents results including nonequilibrium effects, $\Pi_{\text{el}} \neq 0$.

the currents obtained separately for the two states. This approximate treatment is supported by purely electronic as well as inelastic scattering theory calculations that include both electronic states simultaneously.³⁸

We start our discussion with the conductance in the inelastic tunneling regime, shown in Fig. 6. The results exhibit distinct steps at the onset of the inelastic channels corresponding to the excitation of a single vibrational quantum, $\Phi = \Omega_a, \Omega_b, \dots$. For larger voltages, structures related to double excitation processes can be seen. These are highlighted with thin dashed lines. The comparison of the results with and without self energy Π_{el} shows that the renormalization of the vibrational energies, originating from interactions with the electronic degrees of freedom, is negligible.

Next, we consider charge transport through BDBT in the resonant regime. Fig. 7 depicts results of calculations with and without vibrational nonequilibrium effects. In addition, results of purely electronic calculations ($\lambda_\alpha = 0$) are shown. The purely electronic result (dashed line) shows two pronounced steps at voltages where the two electronic states enter the conductance window, respectively. All other smaller structures are due to the energy

dependence of the electronic self energy.³⁸

The inclusion of electronic-vibrational coupling results in a shift of the two major steps from $\Phi = 2.76\text{ V}$ to $\Phi = 2.54\text{ V}$ and from $\Phi = 3.54\text{ V}$ to $\Phi = 3.29\text{ V}$. This shift corresponds to the nuclear reorganization energy in the two electronic states. Furthermore, a number of additional structures appears. For the model considered here, which is dominated by hole transport through occupied states ($\delta = 1$), these structures can be associated with transitions from vibrational states in the neutral molecule to those in the molecular cation. The first four peaks after the onset of the current can be associated with transitions from the vibrational ground state in the neutral molecule to singly excited vibrational states in the cation (i.e. 'emission' processes) corresponding to state A. The fourth of these peaks shows a significant broadening. We devote this broadening to two mixed emission and absorption processes with an energy transfer of $\Delta E = \Omega_d \pm (\Omega_c - \Omega_b)$. For higher voltages, a number of structures can be seen, which are related to vibronic transitions in state B. Thereby, excitation of single vibrational quanta is the dominant process and gives rise to the fundamental peaks at voltages $\Phi = 3.43\text{ V}$, 3.59 V , 3.60 V , 3.71 V . Each of these peaks is accompanied by another peak that results from excitation of an additional quantum of mode (a) at $\Phi = 3.57\text{ V}$, 3.73 V , 3.74 V , 3.85 V . This result demonstrates the strong coupling of mode (a) to state B (cf. Tab. II). Absorptive channels, related to transition from higher excited vibrational states to lower vibrational states, play only a minor role. Three smaller peaks can be assigned to such processes: The first one coincides with the double emission peak at $\Phi = 3.57\text{ V}$ and corresponds to emission of a vibrational quantum with energy Ω_d and absorption of a quantum with energy Ω_a , i.e. $\Delta E = \Omega_d - \Omega_a$. The second peak at $\Phi = 3.46\text{ V}$ involves emission of a vibrational quantum with energy Ω_c and absorption of a quantum with energy Ω_a , i.e. $\Delta E = \Omega_c - \Omega_a$. Finally, the small feature at $\Phi = 3.87\text{ V}$ corresponds to a transition with $\Delta E = \Omega_d + \Omega_c - \Omega_a$.

Electronically mediated mode-mode coupling described by the off-diagonal elements of the self energy matrix Π_{el} has negligible influence on the results (data not shown). In view of the very similar frequencies of modes (b) and (c), this finding is at first glance surprising. The difference of their frequencies, $\Omega_c - \Omega_b$, is, however, large compared to the electronic level broadening Γ_K thus effectively reducing the mode-mode coupling.

In a recent study, we have investigated vibrational effects in charge transport through BDBT employing inelastic scattering theory.³⁸ Inelastic scattering has the advantage that

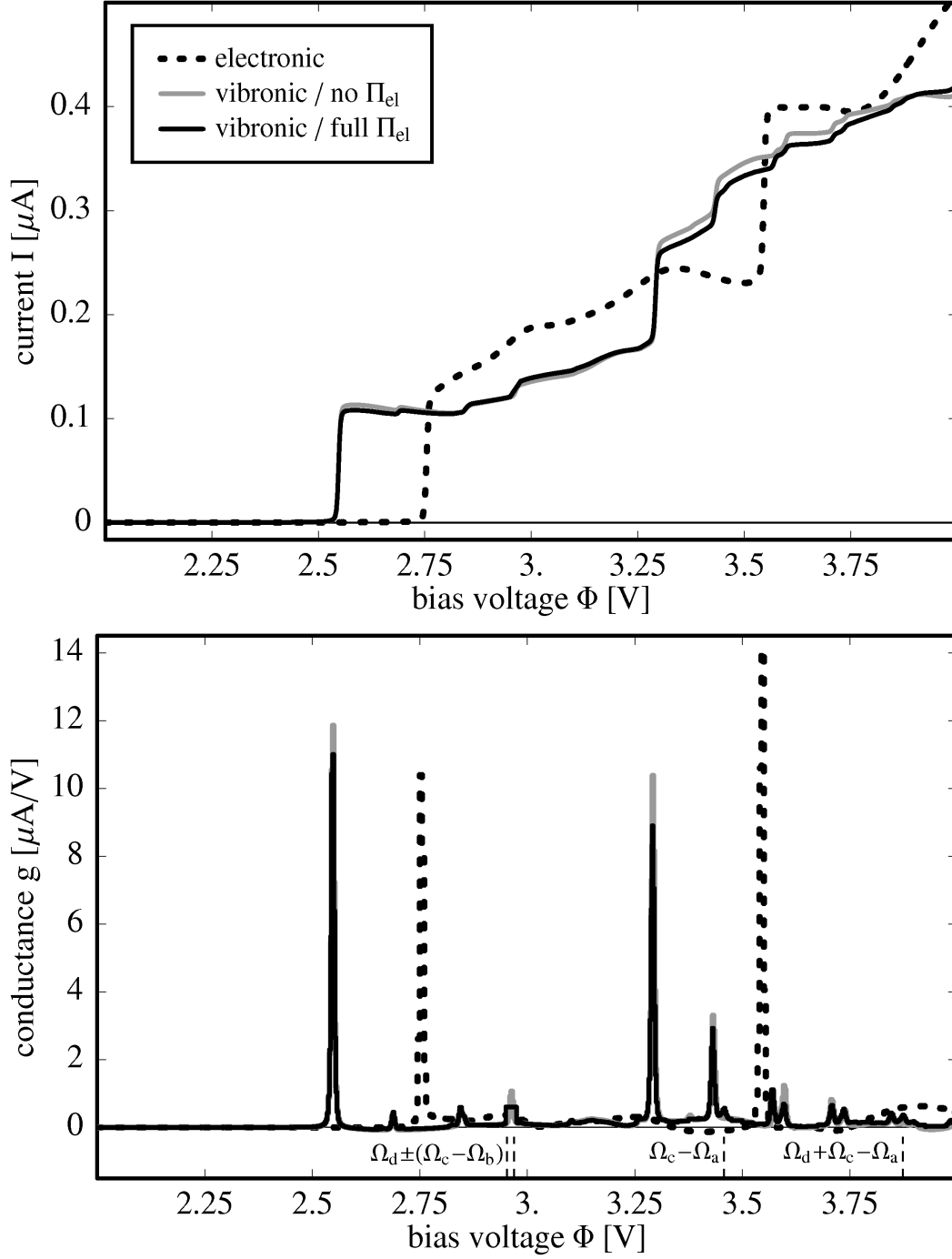


FIG. 7: Current and conductance of the benzenedibutanethiolate molecular junction in the resonant transport regime. The dashed black lines represent results of a purely electronic calculation ($\lambda_\alpha = 0$). Solid gray lines refer to a calculation with vibrations in thermal equilibrium, $\Pi_{\text{el}} = 0$, while solid black lines present results including nonequilibrium effects, $\Pi_{\text{el}} \neq 0$.

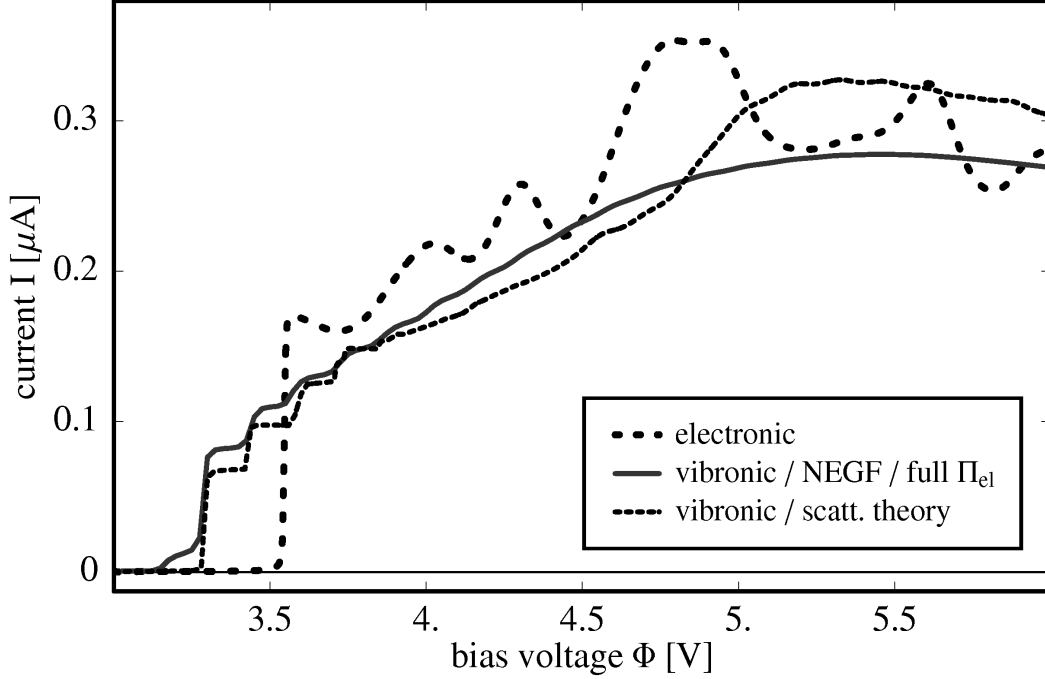


FIG. 8: Comparison of different methods for the current through a benzenedibutanethiolate molecular junction. Shown are results of vibronic calculations employing the nonequilibrium Green's function approach with the full self energy matrix Π_{el} (solid line) and inelastic scattering theory (dotted line).³⁸ The dashed line depicts results of a purely electronic calculation, where both methods give identical results. In contrast to Fig. 7, all calculations include only one electronic state (state B).

the transmission process of a single electron is described numerically exactly. The calculation of the current, however, involves the assumption that the vibrational degrees of freedom of the molecular bridge relax to their equilibrium distribution between two consecutive electron transmission processes. Furthermore, the scattering theory approach cannot account straightforwardly for the nonstationary electronic occupation of the molecular states and, therefore, fails if the molecular levels, which determine the transport, are located close to the Fermi energy.^{38,39} Fig. 8 shows a comparison of results obtained for the current through BDBT employing scattering theory and the nonequilibrium Green's function approach. In addition, results of a purely electronic calculation are shown, where both methods give identical results. To allow a direct comparison, the results have been obtained including only one electronic state on the molecule (state B) and without coupling to the vibrational bath

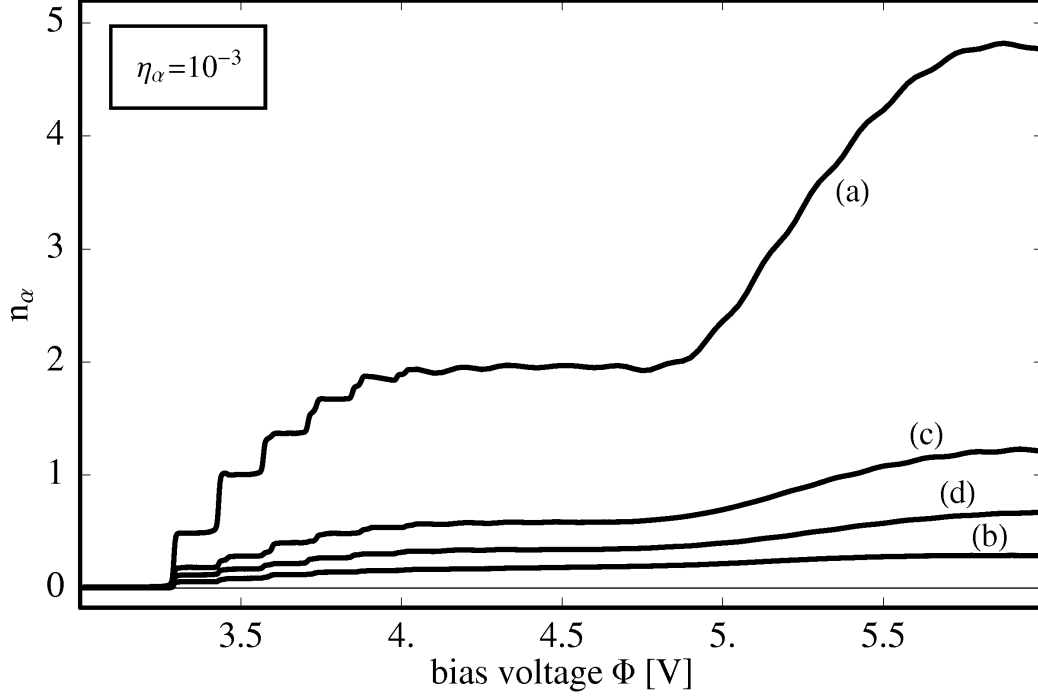


FIG. 9: Nonequilibrium vibrational excitation in charge transport through benzenedibutanethiolate. Shown is the average number of vibrational quanta in the stationary state for modes (a)–(d). The calculation includes only transport through state B and was obtained for a system-bath coupling strength of $\eta_\alpha = 10^{-3}$.

($\eta_\alpha = 0$). Overall, the results show a rather good agreement between the two methods. This is due to the fact that the molecule-lead coupling is rather weak and the energy of state B is located well below the Fermi energy. The major differences are an earlier onset of the current and a smaller current for larger voltages in the Green's function calculation, as well as different heights of the step structures. The earlier onset of the current as well as the different step heights are caused by absorptive vibrational transitions related to the nonequilibrium vibrational distribution and contributions from electron transport. Such processes are not accounted for in scattering theory, which assumes the vibrational degrees of freedom to relax to their equilibrium distribution between two consecutive electron transmission events and (in this case) only considers hole transport. Because the transmission probability is normalized to unity, both results approach each other for larger biases ($\Phi \sim 3.7$ V). Increasing the bias voltage even further, the results start to deviate again. In this regime, current-induced vibrational excitations cannot be neglected and lead to a substantial suppression of

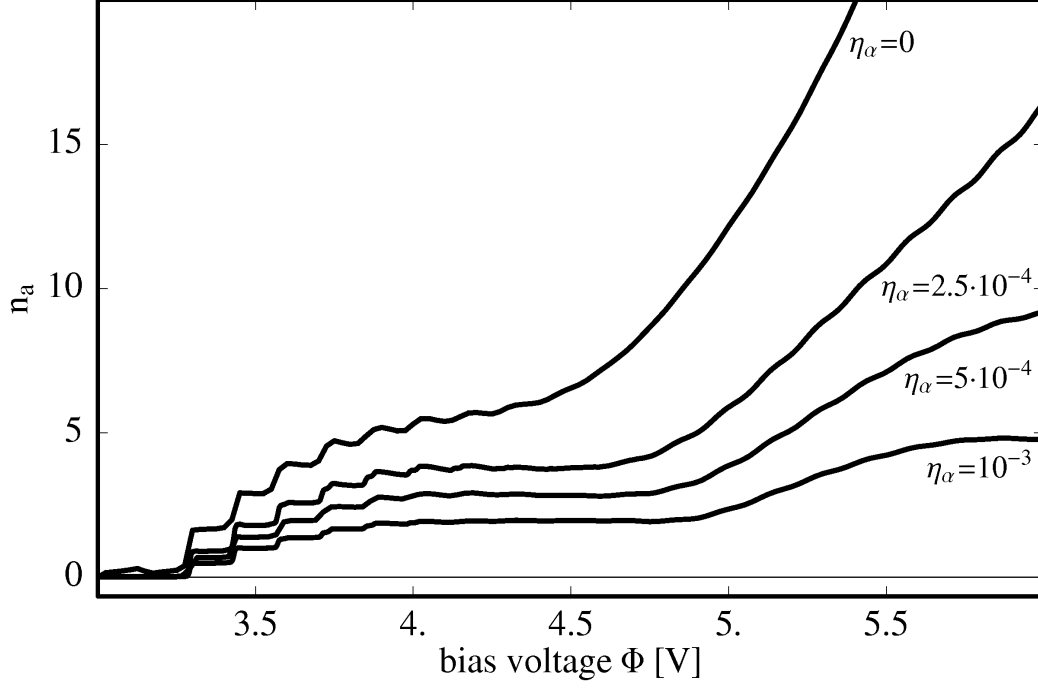


FIG. 10: Nonequilibrium vibrational excitation in charge transport through benzenedibutanethiolate. Shown is the average number of vibrational quanta in the stationary state for mode (a) for different system-bath coupling strengths, η_α . The calculation includes only transport through state B.

the current in the Green's function calculation.⁴⁹

To conclude this section, we consider nonequilibrium vibrational excitation induced by the current through the BDBT junction. Fig. 9 shows the average vibrational excitation of the four modes. It is seen that in the resonant transport regime the current results in significant deviations from the equilibrium distribution. Overall, the amount of excitation of the four modes follows the value of the dimensionless vibronic coupling $\lambda_\alpha/\Omega_\alpha$. In particular mode (a), which has the strongest vibronic coupling, acquires pronounced excitations in the stationary state.

Current-induced excitation of vibrational modes competes with relaxation of vibrational energy due to system-bath coupling and thus depends on the timescale of vibrational relaxation. The influence of the relaxation time is illustrated in Fig. 10 for the strongest coupled mode (a). The results obtained for different values of the system-bath coupling strength, η_α , show the increase of vibrational excitation for longer vibrational relaxation times. In the limit of negligible vibrational relaxation ($\eta_\alpha = 0$), mode (a) is excited to rather high quan-

tum numbers ($n_a > 20$). The corresponding energy is still smaller than typical dissociation energies of a C–C or a C–H bond ($E_{\text{diss}} > 3\text{eV}$). In this regime, however, the harmonic approximation ceases to be valid and anharmonicities should be taken into account.

IV. CONCLUSIONS

In this paper we have studied the effect of multimode vibrational dynamics on charge transport through single molecule junctions. To this end, we have extended a nonequilibrium Green’s function method, developed by Galperin et al.,³³ to treat multiple vibrational modes in transport calculations. This method is based on a polaron transformation of the Hamiltonian and employs perturbation theory within a self-consistent scheme to solve the equations of motion for the nonequilibrium Green’s function. In addition to the simulation of electronic properties such as the electronic current and the conductance, we have also outlined a scheme to calculate the average vibrational excitation in the stationary state using the nonequilibrium Green’s function approach.

The methodology has been applied to two examples: a generic model of a molecular junction with two active vibrational modes as well as charge transport through benzenedibutanethiolate covalently bound to gold electrodes based on a first-principles model. In both cases, the results show that the electronic-vibrational coupling may have significant effects on the current through the molecular junction. The coupling to the vibrational degrees of freedom manifests itself in pronounced structures in the current-voltage characteristic and the differential conductance. Moreover, the current-induced excitation of vibrational modes may result in a significant deviation of the nonequilibrium vibrational distribution from the equilibrium distribution. For modes with similar frequency, mode-mode coupling mediated by the electronic degrees of freedom is of importance. The results show that in this case the full self energy matrix needs to be taken into account in the calculation.

The study in this paper was based on a model, which describes the vibrational degrees of freedom in the harmonic approximation. This approximation is well suited for small amplitude motion and low excitation energies. To investigate the influence of higher vibrational excitation and the possible dissociation of the molecular bridge, the approach has to be extended to include anharmonic effects. This will be the subject of future work.

V. ACKNOWLEDGMENT

We thank Martin Cizek and Wolfgang Domcke for helpful discussions. This work has been supported by the Deutsche Forschungsgemeinschaft, a Grant from the German-Israeli Foundation for Scientific Development (G.I.F.), and the Fonds der chemischen Industrie. Generous allocation of computing time by the Leibniz Rechenzentrum, Munich, is gratefully acknowledged.

APPENDIX A: AVERAGE NUMBER OF VIBRATIONAL EXCITATIONS

In this Appendix, we outline the method used to calculate the average vibrational excitation in the stationary state

$$n_\alpha = \langle a_\alpha^\dagger a_\alpha \rangle_H. \quad (\text{A1})$$

In contrast to the population of the electronic state n_c , the excitation number n_α of mode α is not an invariant of the Lang-Firsov transformation,

$$n_c = \langle c^\dagger c \rangle_H = \langle c^\dagger X X^\dagger c \rangle_{\overline{H}} = \langle c^\dagger c \rangle_{\overline{H}} = \text{Im}[G_c^<(t=0)], \quad (\text{A2})$$

$$n_\alpha = \langle a_\alpha^\dagger a_\alpha \rangle_H = \begin{cases} \langle a_\alpha^\dagger a_\alpha \rangle_{\overline{H}} - \frac{\lambda_\alpha}{\Omega_\alpha} \langle Q_\alpha c^\dagger c \rangle_{\overline{H}} + \frac{\lambda_\alpha^2}{\Omega_\alpha^2} n_c, & \delta=0, \\ \langle a_\alpha^\dagger a_\alpha \rangle_{\overline{H}} - \frac{\lambda_\alpha}{\Omega_\alpha} \langle Q_\alpha c^\dagger c \rangle_{\overline{H}} + \frac{\lambda_\alpha^2}{\Omega_\alpha^2} (1 - n_c) + \frac{\lambda_\alpha}{\Omega_\alpha} \langle Q_\alpha \rangle_{\overline{H}}, & \delta=1. \end{cases} \quad (\text{A3})$$

As a result, we have to calculate four different expectation values to obtain the average excitation number n_α . Thereby, the subscripts H/\overline{H} denote the Hamilton-operator that is used to compute the respective expectation values. In the following we consider only expectation values calculated with \overline{H} , for which the corresponding subscript is omitted from now on.

The third term in Eqs. (A3), $\propto \frac{\lambda_\alpha^2}{\Omega_\alpha^2}$, which can be interpreted as the contribution from polaron formation, can directly be extracted from the electronic Green's function G_c . It only contributes in the resonant transport regime, where n_c deviates significantly from its equilibrium value δ .

The fourth term in Eqs. (A3) for the case $\delta = 1$ contains a single displacement operator

Q_α . For its determination we consider the steady state relations

$$0 = \frac{i\partial \langle \mathbf{P}_a \rangle}{\partial t} = -i\mathbf{W}_a \langle \mathbf{Q}_a \rangle - 2i\mathbf{U} \langle \mathbf{Q}_b \rangle, \quad (\text{A4a})$$

$$0 = \frac{i\partial \langle \mathbf{P}_b \rangle}{\partial t} = -i\mathbf{W}_b \langle \mathbf{Q}_b \rangle - 2i\mathbf{U}^\dagger \langle \mathbf{Q}_a \rangle, \quad (\text{A4b})$$

which result in

$$(\mathbf{1} - 4\mathbf{W}_a^{-1}\mathbf{U}\mathbf{W}_b^{-1}\mathbf{U}^\dagger) \langle \mathbf{Q}_a \rangle = 0. \quad (\text{A5})$$

Because the eigenvalues of the matrix $4\mathbf{W}_a^{-1}\mathbf{U}\mathbf{W}_b^{-1}\mathbf{U}^\dagger$ have to be smaller than unity in order to perform the Lang-Firsov transformation (cf. Sec. II), the expectation value of Q_α vanishes, $\langle Q_\alpha \rangle = 0$.

To treat the second term in Eq. (A3), we consider similar steady-state relations

$$0 = \frac{i\partial \langle \mathbf{P}_a c^\dagger c \rangle}{\partial t} = -i\mathbf{W}_a \langle \mathbf{Q}_a c^\dagger c \rangle - 2i\mathbf{U} \langle \mathbf{Q}_b c^\dagger c \rangle - \sum_{k \in \text{L,R}} V_k \langle \mathbf{P}_a c_k^\dagger c X \rangle + \sum_{k \in \text{L,R}} V_k^* \langle \mathbf{P}_a c^\dagger c_k X^\dagger \rangle, \quad (\text{A6a})$$

$$0 = \frac{i\partial \langle \mathbf{P}_b c^\dagger c \rangle}{\partial t} = -i\mathbf{W}_b \langle \mathbf{Q}_b c^\dagger c \rangle - 2i\mathbf{U}^\dagger \langle \mathbf{Q}_a c^\dagger c \rangle - \sum_{k \in \text{L,R}} V_k \langle \mathbf{P}_b c_k^\dagger c X \rangle + \sum_{k \in \text{L,R}} V_k^* \langle \mathbf{P}_b c^\dagger c_k X^\dagger \rangle. \quad (\text{A6b})$$

Here, additional terms linear in the molecule-lead coupling V_k appear. However, because all expectation values are taken at equal times, these terms cancel each other. This finding is closely related to the existence of a steady-state transport regime that preserves Kirchhoff's law, $I_L = -I_R$. Without the terms linear in V_k , we can follow the same line of argument as for $\langle Q_\alpha \rangle$, and obtain $\langle Q_\alpha c^\dagger c \rangle = 0$.

Finally, to calculate $\langle a_\alpha^\dagger a_\alpha \rangle$, we exploit the momentum correlation matrix \mathbf{D} :

$$\langle a_\alpha^\dagger a_\alpha \rangle = \frac{1}{4} (\langle Q_\alpha Q_\alpha \rangle - \text{Im}[(\mathbf{D}(t=0))_{\alpha\alpha}]) - \frac{1}{2}. \quad (\text{A7})$$

The expectation value $\langle Q_\alpha Q_\alpha \rangle$ can be rewritten in terms of $\langle P_\alpha P_\alpha \rangle$ and $\langle Q_\beta Q_\beta \rangle$. For that purpose, we use the following steady-state relations

$$0 = \frac{i\partial \langle Q_\alpha P_\alpha \rangle}{\partial t} = i\Omega_\alpha \langle P_\alpha P_\alpha \rangle - i\Omega_\alpha \langle Q_\alpha Q_\alpha \rangle - 2i \sum_\beta U_{\alpha\beta} \langle Q_\alpha Q_\beta \rangle, \quad (\text{A8a})$$

$$0 = \frac{i\partial \langle Q_\alpha P_\beta \rangle}{\partial t} = i\Omega_\alpha \langle P_\alpha P_\beta \rangle - i\omega_\beta \langle Q_\alpha Q_\beta \rangle - 2i \sum_{\alpha'} U_{\alpha'\beta} \langle Q_\alpha Q_{\alpha'} \rangle, \quad (\text{A8b})$$

$$0 = \frac{i\partial \langle P_\alpha Q_\beta \rangle}{\partial t} = i\omega_\beta \langle P_\alpha P_\beta \rangle - i\Omega_\alpha \langle Q_\alpha Q_\beta \rangle - 2i \sum_{\beta'} U_{\alpha\beta'} \langle Q_{\beta'} Q_\beta \rangle, \quad (\text{A8c})$$

where, based on the same argument as before, we have disregarded terms linear in V_k . Using these relations, we obtain to second order in the system-bath coupling ($O(U_{\alpha\beta}^2)$)

$$\begin{aligned}\langle Q_\alpha Q_\alpha \rangle &= \langle P_\alpha P_\alpha \rangle + \sum_{\beta, \alpha'} \frac{4\omega_\beta U_{\alpha\beta} U_{\alpha'\beta}}{\Omega_{\alpha'}(\omega_\beta^2 - \Omega_\alpha^2)} \langle P_\alpha P_{\alpha'} \rangle - \sum_{\beta} \frac{4U_{\alpha\beta}^2}{\omega_\beta^2 - \Omega_\alpha^2} \langle Q_\beta Q_\beta \rangle, \\ &\approx \langle P_\alpha P_\alpha \rangle \left(1 + \sum_{\beta} \frac{4\omega_\beta U_{\alpha\beta}^2}{\Omega_\alpha(\omega_\beta^2 - \Omega_\alpha^2)} \right) - \sum_{\beta} \frac{4U_{\alpha\beta}^2}{\omega_\beta^2 - \Omega_\alpha^2} \langle Q_\beta Q_\beta \rangle.\end{aligned}\quad (\text{A9})$$

Thereby, we disregard off-diagonal contributions $\langle P_\alpha P_{\alpha'} \rangle$, which turn out to be negligible. This step is corroborated by considering the special case of degenerate modes (cf. the discussion at the end of Sec. III A).

Inserting Eq. (A9) into Eq. (A7), we obtain the final expression for the excitation number

$$n_\alpha = - \left(A_\alpha + \frac{1}{2} \right) \text{Im}[(\mathbf{D}(t=0))_{\alpha\alpha}] - \left(B_\alpha + \frac{1}{2} \right) + \frac{\lambda_\alpha^2}{\Omega_\alpha^2} \begin{cases} n_c, & \delta = 0, \\ 1 - n_c, & \delta = 1, \end{cases} \quad (\text{A10})$$

with

$$A_\alpha = \sum_{\beta} \frac{U_{\alpha\beta}^2 \omega_\beta}{\Omega_\alpha(\omega_\beta^2 - \Omega_\alpha^2)}, \quad B_\alpha = \sum_{\beta} \frac{U_{\alpha\beta}^2}{(\omega_\beta^2 - \Omega_\alpha^2)} \langle Q_\beta Q_\beta \rangle. \quad (\text{A11})$$

The bath modes remain in thermal equilibrium, for which $\langle Q_\beta Q_\beta \rangle = 1 + 2N_B(\omega_\beta)$ with $N_B(\omega)$ the Bose distribution function.

-
- ¹ M. A. Reed, C. Zhou, C. J. Muller, T. P. Burgin, and J. M. Tour, *Science* **278**, 252 (1997).
 - ² J. Reichert, R. Ochs, D. Beckmann, H. B. Weber, M. Mayor, and H. v. Lohneysen, *Phys. Rev. Lett.* **88**, 176804 (2002).
 - ³ F. Chen, J. Hihath, Z. Huang, X. Li, and N. J. Tao, *Annu. Rev. Phys. Chem.* **58**, 535 (2007).
 - ⁴ Y. Selzer and D. L. Allara, *Annu. Rev. Phys. Chem.* **57**, 593 (2006).
 - ⁵ P. Hänggi, M. A. Ratner, and S. Yaliraki, *Chem. Phys.*, special issue on: "*Processes in Molecular Wires*" **281**, 111 (2002).
 - ⁶ A. Nitzan and M. A. Ratner, *Science* **300**, 1384 (2003).
 - ⁷ G. Cuniberti, G. Fagas, and K. Richter, *Introducing Molecular Electronics* (Springer, Heidelberg, 2005).
 - ⁸ M. Galperin, M. A. Ratner, and A. Nitzan, *J. Phys.: Condens. Matter* **19**, 103201 (2007).
 - ⁹ H. Park, J. Park, A. K. L. Lim, E. H. Anderson, A. P. Alivisatos, and P. L. McEuen, *Nature (London)* **407**, 57 (2000).
 - ¹⁰ A. N. Pasupathy, J. Park, C. Chang, A. V. Soldatov, S. Lebedkin, R. C. Bialczak, J. E. Grose, L. A. K. Donev, J. P. Sethna, D. C. Ralph, et al., *Nano Lett.* **5**, 203 (2005).
 - ¹¹ J. Gaudioso and W. Ho, *J. Am. Chem. Soc.* **123**, 10095 (2001).
 - ¹² J. G. Kushmerick, J. Lazorcik, C. H. Patterson, R. Shashidhar, D. S. Seferos, and G. C. Bazan, *Nano Lett.* **4**, 639 (2004).
 - ¹³ X. H. Qiu, G. V. Nazin, and W. Ho, *Phys. Rev. Lett.* **92**, 206102 (2004).
 - ¹⁴ D. Djukic, K. S. Thygesen, C. Untiedt, R. H. M. Smit, K. W. Jacobsen, and J. M. van Ruitenbeek, *Phys. Rev. B* **71**, 161402(R) (2005).
 - ¹⁵ S. Sapmaz, P. Jarillo-Herrero, Y. M. Blanter, C. Dekker, and H. S. J. van der Zant, *Phys. Rev. Lett.* **96**, 026801 (2006).
 - ¹⁶ W. H. A. Thijssen, D. Djukic, A. F. Otte, R. H. Bremmer, and J. M. van Ruitenbeek, *Phys. Rev. Lett.* **97**, 226806 (2006).
 - ¹⁷ T. Böhler, A. Edtbauer, and E. Scheer, *Phys. Rev. B* **76**, 125432 (2007).
 - ¹⁸ J. J. Parks, A. R. Champagne, G. R. Hutchison, S. Flores-Torres, H. D. Abruna, and D. C. Ralph, *Phys. Rev. Lett.* **99**, 026601 (2007).
 - ¹⁹ N. Ogawa, G. Mikaelian, and W. Ho, *Phys. Rev. Lett.* **98**, 166103 (2007).

- ²⁰ J. Gaudio, L. J. Lauhon, and W. Ho, Phys. Rev. Lett. **85**, 1918 (2000).
- ²¹ E. G. Emberly and G. Kirczenow, Phys. Rev. B **61**, 5740 (2000).
- ²² D. Boese and H. Schoeller, Europhys. Lett. **54**, 668 (2001).
- ²³ H. Ness, S. A. Shevlin, and A. J. Fisher, Phys. Rev. B **63**, 125422 (2001).
- ²⁴ A. Troisi, M. A. Ratner, and A. Nitzan, J. Chem. Phys. **118**, 6072 (2003).
- ²⁵ A. Pecchia and A. Di Carlo, Nano Lett. **4**, 2109 (2004).
- ²⁶ Y. Chen, M. Zwolak, and M. Di Ventra, Nano Lett. **5**, 813 (2005).
- ²⁷ V. May and O. Kühn, Chem. Phys. Lett. **420**, 192 (2006).
- ²⁸ J. Lehmann, S. Kohler, V. May, and P. Hänggi, J. Chem. Phys. **121**, 2278 (2004).
- ²⁹ J. Koch and F. von Oppen, Phys. Rev. Lett. **94**, 206804 (2005).
- ³⁰ M. R. Wegewijs and K. C. Nowack, New J. Phys. **7**, 239 (2005).
- ³¹ J. Jiang, M. Kula, and Y. Luo, J. Chem. Phys. **124**, 34708 (2006).
- ³² D. A. Ryndyk, M. Hartung, and G. Cuniberti, Phys. Rev. B **73**, 045420 (2006).
- ³³ M. Galperin, A. Nitzan, and M. A. Ratner, Phys. Rev. B **73**, 045314 (2006).
- ³⁴ A. Gagliardi, G. C. Solomon, A. Pecchia, T. Frauenheim, A. Di Carlo, N. S. Hush, and J. R. Reimers, Phys. Rev. B **75**, 174306 (2007).
- ³⁵ N. Sergueev, A. A. Demkov, and H. Guo, Phys. Rev. B **75**, 233418 (2007).
- ³⁶ T. Frederiksen, M. Paulsson, M. Brandbyge, and A.-P. Jauho, Phys. Rev. B **75**, 205413 (2007).
- ³⁷ M. Caspary-Toroker and U. Peskin, J. Chem. Phys. **127**, 154706 (2007).
- ³⁸ C. Benesch, M. Cizek, J. Klimes, M. Thoss, and W. Domcke, arXiv:0712.3690 (2008).
- ³⁹ M. Cizek, M. Thoss, and W. Domcke, Phys. Rev. B **70**, 125406 (2004).
- ⁴⁰ For a more detailed discussion of the Hamiltonian, see Ref. 38.
- ⁴¹ U. Weiss, *Quantum Dissipative Systems* (World Scientific, Singapore, 1999), 2nd ed.
- ⁴² G. D. Mahan, *Many-Particle Physics* (Plenum Press, 1981).
- ⁴³ I. G. Lang and Y. A. Firsov, Sov. Phys. JETP **16**, 1301 (1963).
- ⁴⁴ L. V. Keldysh, Sov. Phys. JETP **20**, 1018 (1965).
- ⁴⁵ H. Haug and A.-P. Jauho, *Quantum Kinetics in Transport and Optics of Semiconductors* (Springer, Berlin, 1996).
- ⁴⁶ D. C. Langreth, *Linear and Nonlinear Electron Transport in Solids* (Plenum Press, New York, 1976).
- ⁴⁷ Y. Meir and N. S. Wingreen, Phys. Rev. Lett. **68**, 2512 (1992).

- ⁴⁸ A.-P. Jauho, N. S. Wingreen, and Y. Meir, Phys. Rev. B **50**, 5528 (1994).
- ⁴⁹ A. Mitra, I. Aleiner, and A. J. Millis, Phys. Rev. B **69**, 245302 (2004).
- ⁵⁰ C. Benesch, M. Cizek, M. Thoss, and W. Domcke, Chem. Phys. Lett. **430**, 355 (2006).